J. of Electromagn. Waves and Appl., Vol. 20, No. 6, 827–839, 2006

LORENTZ FORCE ON DIELECTRIC AND MAGNETIC PARTICLES

B. A. Kemp, T. M. Grzegorczyk, and J. A. Kong

Research Laboratory of Electronics
Massachusetts Institute of Technology
77 Massachusetts Ave., 26-305, MA 02139, USA

Abstract—The well-known momentum conservation theorem is derived specifically for time-harmonic fields and is applied to calculate the radiation pressure on 2-D particles modeled as infinite dielectric and magnetic cylinders. The force calculation results from the divergence of the Maxwell stress tensor and is compared favorably via examples with the direct application of Lorentz force to bound currents and charges. The application of the momentum conservation theorem is shown to have the advantage of less computation, reducing the surface integration of the Lorentz force density to a line integral of the Maxwell stress tensor. The Lorentz force is applied to compute the force density throughout the particles, which demonstrates regions of compression and tension within the medium. Further comparison of the two force calculation methods is provided by the calculation of radiation pressure on a magnetic particle, which has not been previously published. The fields are found by application of the Mie theory along with the Foldy-Lax equations, which model interactions of multiple particles.

1. INTRODUCTION

The first observation of optical momentum transfer to small particles in 1970 [1] prompted further experimental demonstrations of radiation pressure such as optical levitation [2], radiation pressure on a liquid surface [3], and the single-beam optical trap [4], to name a few. Subsequently, theoretical models have been developed to describe the experimental results and predict new phenomena, for example [5–9]. However, the theory of radiation pressure is not new. In fact, the transfer of optical momentum to media was known by Poynting [10] from the application of the electromagnetic wave theory of light. Still,

ongoing work seeks to model the distribution of force on media by electromagnetic waves [11–14].

The divergence of the Maxwell stress tensor [15] provides an established method for calculating the radiation pressure on a dielectric surface via the application of the momentum conservation theorem [16]. An alternate method for the calculation of radiation pressure on material media by the direct application of the Lorentz law has been recently reported [12]. The method allows for the computation of force density at any point inside a dielectric [13] by the application of the Lorentz force to bound currents distributed throughout the medium and bound charges at the material surface, and the method has been extended to include contributions from magnetic media [14]. A comprehensive comparison of the two methods applied to particles has not been previously published, and, consequently, there exists some doubt in regard to the applicability of one method or the other.

In the present paper, we compare the force exerted on 2-D dielectric cylinders as calculated from the divergence of the Maxwell stress tensor and the distributed Lorentz force. First, the total time average force as given by the divergence of the Maxwell stress tensor [16] is derived from the Lorentz law and the Maxwell equations for time harmonic fields. We demonstrate the numerical efficiency of the stress tensor method by computing the force on a 2-D dielectric particle represented by an infinite cylinder submitted to multiple plane waves. Second, we give the formulation for the distributed Lorentz force as applied to dielectric and magnetic media [12–14]. The numerical integration of the distributed Lorentz force over the 2-D particle cross-section area demonstrates equivalent results, although the convergence is shown to be much slower than the stress tensor line integration. Third, both the Maxwell stress tensor and the distributed Lorentz force methods are applied to two closely spaced particles in the three plane wave interference pattern, the former method exhibiting robustness with respect to choice of integration path and the latter method providing a 2-D map of the Lorentz force density distribution within the particles. Finally, the first theoretical demonstration of the Lorentz force applied to bound magnetic charges and currents in a 2-D particle is presented.

2. MAXWELL STRESS TENSOR

The momentum conservation theorem [16] relates the total force on a material object in terms of the momentum of the incident and scattered fields at all times. It is derived from the Lorentz force law and the Maxwell equations. In the case of time-harmonic fields, the

time-average force on a material body can be calculated from a single divergence integral. The proof of this fact is shown by derivation of the momentum conservation theorem with the only assumption that all fields have $e^{-i\omega t}$ dependence.

The Lorentz force provides the fundamental relationship between electromagnetic fields and the mechanical force on charges and currents [16]. The time average Lorentz force is given in terms of the electric field strength $\bar{E}$ and magnetic flux density $\bar{B}$ by

$$\bar{f} = \frac{1}{2} Re\Big\{\rho \bar{E}^* + \bar{J} \times \bar{B}^*\Big\}, \tag{1}$$

where ρ and $\bar{J}$ represent the electric charge and current, respectively, $Re\{\}$ represents the real part of a complex quantity, and $(^*)$ denotes the complex conjugate. The Maxwell Equations

$$\begin{aligned} \rho &= \nabla \cdot \bar{D} \\ \bar{J} &= \nabla \times \bar{H} + i\omega \bar{D} \end{aligned} \tag{2}$$

relate the sources ρ and $\bar{J}$ to the electric flux density $\bar{D}$ and magnetic field strength $\bar{H}$. Substitution yields

$$\bar{f} = \frac{1}{2} Re\Big\{(\nabla \cdot \bar{D})\bar{E}^* + (\nabla \times \bar{H}) \times \bar{B}^* - \bar{D} \times (i\omega \bar{B})^*\Big\}. \tag{3}$$

After applying the remaining two Maxwell equations

$$\begin{aligned} 0 &= \nabla \cdot \bar{B} \\ i\omega \bar{B} &= \nabla \times \bar{E}, \end{aligned} \tag{4}$$

the force can by expressed as

$$\bar{f} = \frac{1}{2} Re\Big\{(\nabla \cdot \bar{D})\bar{E}^* + (\nabla \times \bar{E}^*) \times \bar{D} + (\nabla \cdot \bar{B}^*)\bar{H} + (\nabla \times \bar{H}) \times \bar{B}^*\Big\}. \tag{5}$$

The momentum conservation theorem for time harmonic fields is reduced to

$$\bar{f} = -\frac{1}{2} Re\Big\{\nabla \cdot \bar{\bar{T}}(\bar{r})\Big\}, \tag{6}$$

where $\bar{f}$ is the time average force density in N/m^3, and the Maxwell stress tensor is [16]

$$\bar{\bar{T}}(\bar{r}) = \frac{1}{2}\left(\bar{D} \cdot \bar{E}^* + \bar{B}^* \cdot \bar{H}\right)\bar{\bar{I}} - \bar{D}\bar{E}^* - \bar{B}^*\bar{H}. \tag{7}$$

In (7), $\bar{D}\bar{E}^*$ and $\bar{B}^*\bar{H}$ are dyadic products and $\bar{\bar{I}}$ is the (3×3) identity matrix. By integration over a volume V enclosed by a surface S and

application of the divergence theorem, the total force $\bar{F}$ on the material enclosed by S is given by

$$\bar{F} = -\frac{1}{2} Re\left\{ \oint_S dS \left(\hat{n} \cdot \bar{\bar{T}}(\bar{r}) \right) \right\}, \tag{8}$$

where $\hat{n}$ is the outward normal to the surface S. When applying (8) to calculate the force on a material object, the stress tensor in (7) is integrated over a surface chosen to completely enclose the object.

We consider the two-dimensional (2-D) problem of a circular cylinder incident by three TE plane waves. The incident electric field pattern $|\bar{E}|$ shown in Fig. 1 is due to three plane waves with free space wavelength $\lambda_0 = 532$ [nm] incident in the (xy) plane at angles $\phi = \{\pi/2, 7\pi/6, 11\pi/6\}$ [rad] with the electric field polarized in the $\hat{z}$-direction. The polystyrene cylinder ($\epsilon_p = 2.56\epsilon_0$) has a radius of $a = 0.3\lambda_0$ and is centered at $(x_0, y_0) = (0, 100)$ [nm] in a background of water ($\epsilon_b = 1.69\epsilon_0$). The total field is obtained as the superposition of incident and scattered fields, the latter is calculated from application of the Mie theory [8, 9].

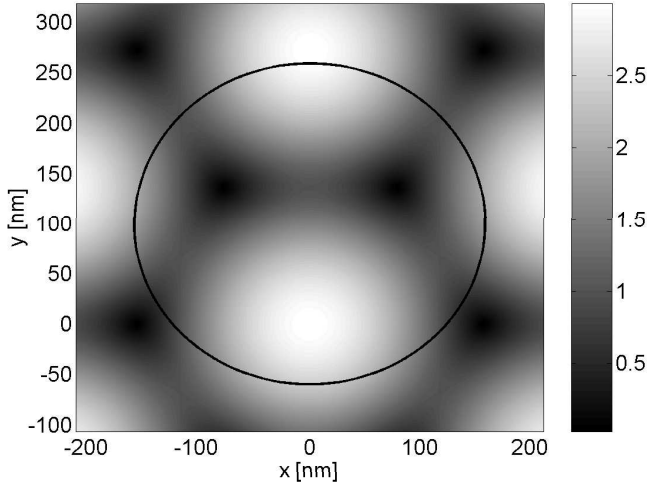

Figure 1. Incident electric field magnitude [V/m] due to three plane waves of free space wavelength $\lambda_0 = 532\,\text{nm}$ propagating at angles $\{\pi/2, 7\pi/6, 11\pi/6\}$ rad. The overlayed 2D particle is a cylinder ($\epsilon_p = 2.56\epsilon_0$) of radius $a = 0.3\lambda_0$ and infinite length in z with center position $(x_0, y_0) = (0, 100)$ [nm]. The background medium is characterized by $\epsilon_b = 1.69\epsilon_0$.

To calculate the total force on the cylinder shown in Fig. 1, the Maxwell stress tensor is applied to the total field. For the 2-D problem, the divergence of the stress tensor is computed by a line integral, which we evaluate by simple numerical integration. The path chosen is a circle of radius R concentric with the particle and the integration steps ($R\Delta\phi$) are assumed constant. The numerical integration is computed by

$$\bar{F} = -\frac{1}{2} Re \left\{ \int_0^{2\pi} \hat{n} \cdot \bar{\bar{T}}(R,\phi) R d\phi \right\} \approx -R\Delta\phi \sum_{n=1}^{N} \frac{1}{2} Re \left\{ \hat{n} \cdot \bar{\bar{T}}(R,\phi[n]) \right\}, \tag{9}$$

where N represents the total number of integration points and the values of $\phi[n]$ result from the discretization of $\phi \in [0, 2\pi]$. Figure 2 shows the force versus the number of integration points for an integration radius of $R = 1.01a$. The results show that the integration converges rapidly. Because the force is calculated by a divergence integral, the result does not depend on the value of R, provided enough integration points are chosen. To confirm this, the force was calculated

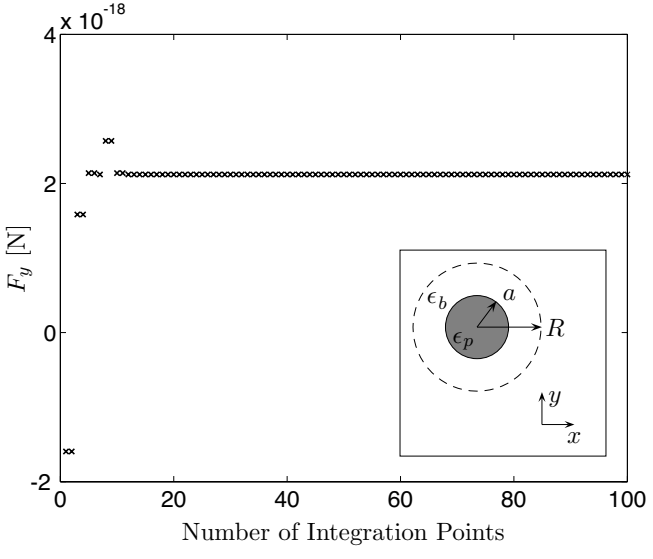

Figure 2. $\hat{y}$-directed force F_y versus the number of integration points used in the application of the Maxwell stress tensor in Eq. (9). The integration path, shown by the inset diagram, is a circle of radius of $R = 1.01a$ concentric with the cylinder of radius $a = 0.3\lambda_0$. The configuration is the same as shown in Fig. 1.

for various choices of integration radius yielding zero for all $R < a$ and $\bar{F} = \hat{y}2.1190 \cdot 10^{-18}$ [N/m] for all $R > a$, which is in agreement with the value reported by [14].

3. LORENTZ FORCE ON BOUND CURRENTS AND CHARGES

The Lorentz force can be applied directly to bound currents and charges in a lossless medium [14]. The bulk force density in [N/m^3] is computed throughout the medium by

$$\bar{f}_{bulk} = \frac{1}{2} Re\{-i\omega \bar{P}_e \times \bar{B}^* - i\omega \bar{P}_m \times \bar{D}^*\}, \tag{10}$$

where the electric polarization $\bar{P}_e = (\epsilon_p - \epsilon_b)\bar{E}$ and the magnetic polarization $\bar{P}_m = -(\mu_p - \mu_b)\bar{H}$ are given in terms of the background constitutive parameters (μ_b, ϵ_b) and the particle constitutive parameters (μ_p, ϵ_p). The surface force density in [N/m^2] is given by

$$\bar{f}_{surf} = \frac{1}{2} Re\{\rho_e \bar{E}^*_{avg} + \rho_m \bar{H}^*_{avg}\}, \tag{11}$$

where the bound electric surface charge density is $\rho_e = \hat{n} \cdot (\bar{E}_1 - \bar{E}_0)\epsilon_b$ [12], the bound magnetic surface charge density is $\rho_m = \hat{n} \cdot (\bar{H}_1 - \bar{H}_0)\mu_b$ [14], and the unit vector $\hat{n}$ is an outward pointing normal to the surface. The fields $(\bar{E}_0, \bar{H}_0)$ and $(\bar{E}_1, \bar{H}_1)$ are the total fields just inside the particle and outside the particle, respectively, and the fields in (11) are given by $\bar{E}_{avg} = (\bar{E}_1 + \bar{E}_0)/2$ and $\bar{H}_{avg} = (\bar{H}_1 + \bar{H}_0)/2$.

The distributed Lorentz force is applied to the problem of Fig. 1. Because TE polarized waves are incident upon a dielectric particle, the bound charges at the surface are zero and the total force $\bar{F}$ is obtained by integrating the bulk Lorentz force density $\bar{f}_{bulk}$ over the cross section of the cylinder. The numerical integration is performed by summing the contribution from M discrete area elements. The area elements $\Delta A = \Delta x \Delta y$ are taken to be identical so that the numerical integration is

$$\bar{F} = \iint_S dA \frac{1}{2} Re\{\bar{f}_{bulk}\} \approx \Delta A \sum_{m=1}^{M} \frac{1}{2} Re\{-i\omega \bar{P}_e[m] \times \mu_0 \bar{H}^*[m]\}, \tag{12}$$

where the dielectric polarization $\bar{P}_e[m]$ and magnetic field $\bar{H}[m]$ are evaluated at each point indexed by m in the cross section of the cylinder. The $\hat{y}$-directed force is plotted in Fig. 3 versus the number of integration points. The integral converges much slower than the

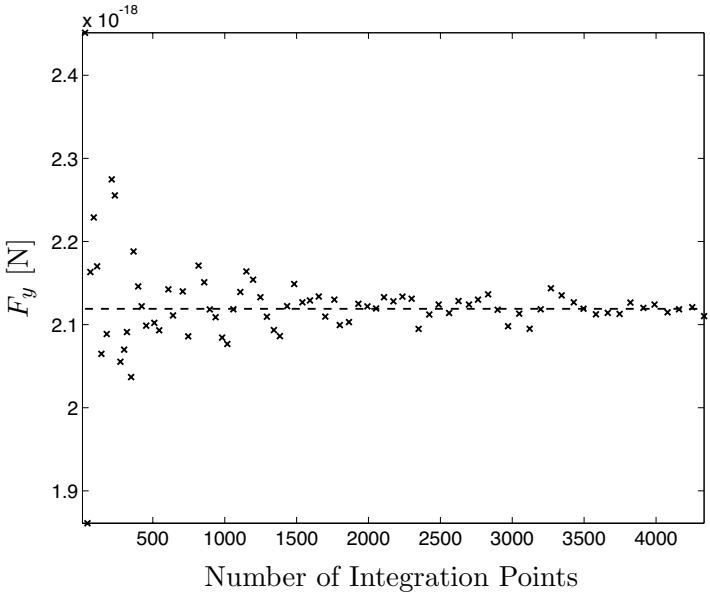

Figure 3. $\hat{y}$-directed force F_y versus the number of integration points for the direct application of the Lorentz force of (12). The configuration is the same as shown in Fig. 1. The dashed line is the force computed from the stress tensor of (9) with 100 numerical integration points on a concentric circle of radius $R = 1.01a$.

line integral applied to the stress tensor, however the resulting force is $\bar{F} = \hat{y}2.1191 \cdot 10^{-18}$ [N/m], thus matching the result from the Maxwell stress tensor.

4. FORCE ON MULTIPLE DIELECTRIC PARTICLES

The Mie theory and the Foldy-Lax multiple scattering equations are applied to calculate the force on multiple particles incident by a known electromagnetic field [8, 9]. We consider the same incident field shown in Fig. 1 with two identical dielectric particles centered at $(x, y) = (0, 100)$ [nm] and $(x, y) = (0, -300)$ [nm] as shown in Fig. 4. As before, the 2-D polystyrene particles are modeled as infinite dielectric cylinders ($\epsilon_p = 2.56\epsilon_0$) in water ($\epsilon_b = 1.69\epsilon_0$) with radius $a = 0.3\lambda_0$.

The Maxwell stress tensor is applied to calculate the force on each particle by taking an integration path that just encloses each particle as shown in Fig. 4. The force for the particle at $(x, y) = (0, 100)$ [nm] is $\bar{F} = \hat{y}1.6517 \cdot 10^{-18}$ [N/m], and the force on the particle at

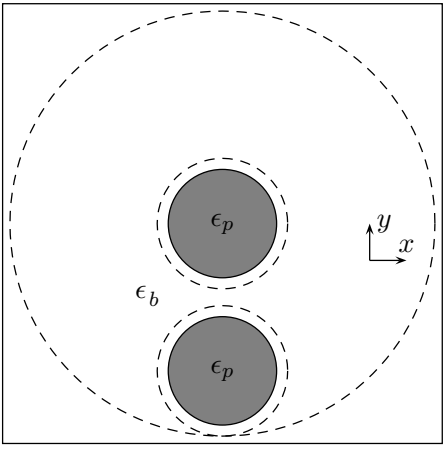

Figure 4. Two particles centered at $(x, y) = (100, 0)$, $(-300, 0)$ [nm] are subject to the incident field pattern of Fig. 1. The integration paths for the Maxwell stress tensor applied to the two particles are shown by the dotted lines. The sum of the forces on the two individual particles obtained by the smaller two integration circles is equal to the force obtained by integrating over the large circular integration path.

$(x, y) = (0, -300)\,[\text{nm}]$ is $\bar{F} = -\hat{y}1.4490 \cdot 10^{-18}\,[\text{N/m}]$. By taking the integration path surrounding both particles, the total force on the system composed of both particles is $\bar{F} = \hat{y}2.0269 \cdot 10^{-19}$ [N/m], which agrees with the sum of the individual forces. This example demonstrates that the divergence of the stress tensor gives the total force on all currents and charges enclosed by the integration path and that the integration path needs not be concentric with the material bodies.

For comparison with the stress tensor method, the Lorentz force is applied to bound electric currents in both particles. The distribution of force densities are shown in Fig. 5. Although the $\hat{x}$-directed force integrates to zero for both particles due to symmetry, it can be seen that the local force densities vary throughout the particle. These forces act in compression or tension in the various regions of the particle. The total force on each particle is found by integration of the local force densities throughout the particles. The force for the particle at $(x, y) = (0, 100)\,[\text{nm}]$ is $\bar{F} = \hat{y}1.6500 \cdot 10^{-18}\,[\text{N/m}]$ using $17,534$ integration points, and the total force on the particle at $(x, y) = (0, -300)\,[\text{nm}]$ is $\bar{F} = -\hat{y}1.4523 \cdot 10^{-18}\,[\text{N/m}]$ using $17,530$ integration points, which is agreement with the results of the Maxwell stress tensor divergence.

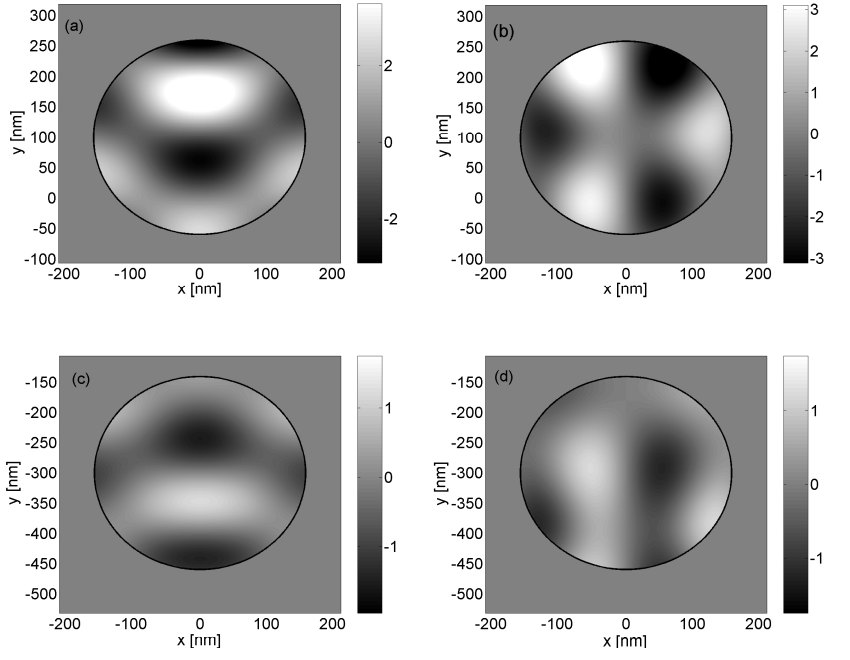

Figure 5. Lorentz force density $[10^{-4}\,\mathrm{N/m^3}]$ for two particles positioned at $(x, y) = (100, 0), (-300, 0)\,[\mathrm{nm}]$ illuminated by the three plane waves of free space wavelength $\lambda_0 = 532\,\mathrm{nm}$ as shown in Fig. 1. The top plots are (a) $\hat{y}$-directed force f_y and (b) $\hat{x}$-directed force f_x for the particle at $(x, y) = (0, 100)\,[\mathrm{nm}]$. The bottom plots are (c) $\hat{y}$-directed force f_y and (d) $\hat{x}$-directed force f_x for the particle at $(x, y) = (0, -300)\,[\mathrm{nm}]$. The total Lorentz force on the particles is obtained by summation of the force densities on the particle at $(x, y) = (0, 100)\,[\mathrm{nm}]$ $(\bar{F} = \hat{y}1.6500 \cdot 10^{-18}\,[\mathrm{N/m}])$ and the particle at $(x, y) = (0, -300)\,[\mathrm{nm}]$ $(\bar{F} = -\hat{y}1.4523 \cdot 10^{-18}\,[\mathrm{N/m}])$. For both particles, the $\hat{x}$-directed force is zero due to symmetry.

5. RADIATION PRESSURE ON A MAGNETIC PARTICLE

The Lorentz force has been previously applied to bound magnetic charges and currents to calculate the radiation pressure on a magnetic slab [14]. However, the method has not been used to determine the force on magnetic particles. In this section, we calculate the radiation pressure on a 2-D magnetic particle represented by an infinite cylinder incident by a single TE plane wave.

The incident plane wave $\bar{E}_i = \hat{z}E_i e^{ik_0 x}$ propagates in free space (ϵ_0, μ_0) with a wavelength $\lambda_0 = 2\pi/k_0 = 640\,[\text{nm}]$. The 2-D magnetic particles $(\epsilon_0, 3\mu_0)$ are infinite in the $\hat{z}$-direction, with radius a. The Maxwell stress tensor and the distributed Lorentz force methods are applied to calculate the total force on the particles. The direct application of the Lorentz force requires the model of bound magnetic currents $\bar{M}_b = -i\omega\bar{P}_m$ in (10) and bound magnetic surface charges ρ_m in (11). Agreement between the two methods is shown in Fig. 6 as a function of particle radius. The oscillations in force are a result of internal resonances, which is also evident for the case of dielectric and magnetic slabs incident by plane waves [14].

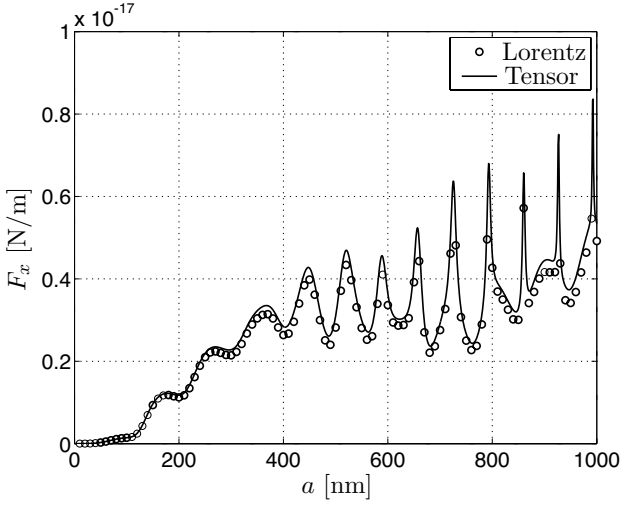

Figure 6. Radiation pressure on a magnetic cylinder ($\mu_p = 3\mu_0,\ \epsilon_p = \epsilon_0$) versus the radius a. The TE plane wave propagates in the $\hat{x}$-direction in free space ($\mu_b = \mu_0,\ \epsilon_b = \epsilon_0$), and the wavelength is 640 [nm]. The force is calculated by the divergence of the stress tensor (line) and the Lorentz force on bound currents and charges (markers).

There are noticeable differences between the results of the two methods for larger values of a as shown in Fig. 6. This is due to increased spacial variations in force distribution for particles on the order of a wavelength or larger. The slow convergence of the total Lorentz force has been observed for small dielectric particles as shown in Fig. 3 and becomes a major obstacle for obtaining many digits of accuracy from the Lorentz force for large particles. To illustrate this point, we compare the force calculated for the magnetic particle with radius $a = 1000\,\text{nm}$ with various number of integration points N in

Table 1. Radiation pressure on a magnetic particle ($a = 1000\,[\mathrm{nm}]$).

Number of Integration Points	Total Lorentz Force F_x
25,952	$4.8177 \cdot 10^{-18}$ [N/m]
103,336	$4.9175 \cdot 10^{-18}$ [N/m]
282,868	$4.9498 \cdot 10^{-18}$ [N/m]

Table 1. For each calculation, 200 points are used for the calculation of force on bound surface charges, which was determined to be enough for the number of significant digits reported. The force obtained from the stress tensor approach is $5.3524 \cdot 10^{-18}$ [N/m], which converges within 100 points. It is clear that for this particular case, the total Lorentz force converges so slowly that it could hinder studies involving many variables or multiple particles [8, 9]. For many applications, however, the Lorentz force is useful for getting a picture of force distribution inside the particle, while the divergence of the stress tensor is much more efficient for obtaining the total force on the particle.

6. CONCLUSIONS

We have calculated the radiation pressure on 2-D particles from both the divergence of the Maxwell stress tensor and the direct application of the Lorentz force to bound currents and charges. The Maxwell stress tensor was derived for time harmonic fields from the Lorentz force and the Maxwell equations. The Lorentz force is applied directly to bound currents and charges used to model dielectric and magnetic materials. The advantage of the stress tensor approach for force calculation on 2-D particles, is that it reduces a combination of surface integral over the bulk force density $\bar{f}_{bulk}$ in (10) and a line integral over the surface force density $\bar{f}_{surf}$ in (11) to the line integral (8) over the Maxwell stress tensor in (7). This reduction in computation has been demonstrated by example. The Lorentz force, however, can give the force distribution throughout the particle. Such distributions can be important when optical forces are applied to sensitive objects such as in biological applications. For large particles, the total force may be difficult to obtain accurately from the Lorentz force density, which we illustrated by calculating the radiation pressure on a magnetic particle. In applications of optical binding [8] such as building optical matter [17], the Lorentz force can be applied to map force distributions within particles, while the stress tensor approach can be used to find the total force on the particle lattice.

ACKNOWLEDGMENT

This work is sponsored by the Department of the Air Force under Air Force Contract FA8721-05-C-0002. Opinions, interpretations, conclusions and recommendations are those of the author and are not necessarily endorsed by the United States Government.

REFERENCES

1. Ashkin, A., "Acceleration and trapping of particles by radiation pressure," *Phys. Rev. Lett.*, Vol. 26, 156–159, 1970.
2. Ashkin, A. and J. M. Dziedzic, "Optical levitation by radiation pressure," *Appl. Phys. Lett.*, Vol. 19, No. 8, 283–285, 1971.
3. Ashkin, A. and J. M. Dziedzic, "Radiation pressure on a free liquid surface," *Phys. Rev. Lett.*, Vol. 30, No. 4, 139–142, 1973.
4. Ashkin, A., J. M. Dziedzic, J. E. Bjorkholm, and S. Chu, "Observation of a single-beam gradient force optical trap for dielectric particles," *Opt. Lett.*, Vol. 11, No. 5, 288–290, 1986.
5. Gordon, J. P., "Radiation forces and momenta in dielectric media," *Phys. Rev. A*, Vol. 8, No. 1, 14–21, 1973.
6. Harada, Y. and T. Asakura, "Radiation forces on a dielectric sphere in the Rayleigh scattering regime," *Optics Comm.*, Vol. 124, 529–541, 1996.
7. Rockstuhl, C. and H. P. Herzig, "Rigorous diffraction theory applied to the analysis of the optical force on elliptical nano- and micro-cylinders," *J. of Optics A: Pure Appl. Opt.*, Vol. 6, No. 10, 921–931, 2004.
8. Grzegorczyk, T. M., B. A. Kemp, and J. A. Kong, "Trapping and binding of an arbitrary number of cylindrical particles in an in-plane electromagnetic field," *J. Opt. Soc. Am. A*, submitted to publication.
9. Grzegorczyk, T. M., B. A. Kemp, and J. A. Kong, "Stable optical trapping based on optical binding forces," *Phys. Rev. Lett.*, submitted to publication.
10. Poynting, J. H., "Tangential stress of light obliquely incident on absorbing surface," *Philosophical Magazine*, Vol. 9, 169–171, 1905.
11. Loudon, R., "Theory of radiation pressure on dielectric surfaces," *J. Mod. Opt.*, Vol. 49, 821–838, 2002.
12. Mansuripur, M., "Radiation pressure and the linear momentum of the electromagnetic field," *Opt. Express*, Vol. 12, 5375–5401, 2004.

13. Zakharian, A. R., M. Mansuripur, and J. V. Moloney, "Radiation pressure and the distribution of electromagnetic force in a dielectric media," *Opt. Express*, Vol. 13, 2321–2336, 2005.
14. Kemp, B. A., T. M. Grzegorczyk, and J. A. Kong, "Ab initio study of the radiation pressure on dielectric and magnetic media," *Opt. Express*, Vol. 13, 9280–9291, 2005.
15. Stratton, J. A., *Electromagnetic Theory*, McGraw-Hill, 1941 (ISBN 0-07-062150-0).
16. Kong, J. A., *Electromagnetic Wave Theory*, EMW, Cambridge, 2005 (ISBN 0-9668143-9-8).
17. Burns, M. M., J. M. Fournier, and J. A. Golovchenko, "Optical matter: Crystallization and binding in intense optical fields," *Science*, Vol. 249, 749–754, 1990.